Relationship between Heat Transfer and Pressure Drop of Porous Materials

Fukuda, Kenji
Department of Energy Conversion Engineering, Interdisciplinary Graduate School of Engineering Sciences, Kyushu University

Kondoh, Tetsuya
Toa University

Hasegawa, Shu
Kurume National College of Technology

https://doi.org/10.15017/17272

出版情報：九州大学大学院総合理工学報告. 14 (2), pp.213-223, 1992-09-01. 九州大学大学院総合理工学研究科
バージョン：
権利関係：

九州大学大学院総合理工学研究科報告
第14巻 第2号 213-223頁 平成4年6月

Engineering Sciences Reports, Kyushu University
(KYUSHU DAIGAKU SOGORIKOGAKU KENKYUKA HOKOKU)
Vol. 14, No. 2, pp. 213-223, SEPT 1992

Relationship between Heat Transfer and Pressure Drop of Porous Materials

Kenji FUKUDA*, Tetsuya KONDOH** and Shu HASEGAWA***

(Received May 29, 1992)

An experimental study has been carried out to investigate into the similarity rule which might exist between the heat transfer and the pressure drop characteristics of the fluid flow through porous materials. The steady heating method is applied to measure the heat transfer coefficient of the foamed metals and the wire lattices, and the transient heating method for the packed beds of glass beads, etc.

From the pressure drop data a proper characteristic length is derived with which the Reynolds number (Re) and the Nusselt number (Nu) are defined. It is shown that a universal law or a similarity rule $Nu = f(Re)$ exist applicable to various porous materials.

1. Introduction

Porous materials are used in many engineering components such as the fixed bed for chemical reactors, regenerator of the Stirling engine, the pebble bed of the high temperature gas cooled nuclear reactor etc.

In general, heat transfer and pressure drop characteristics of the porous materials are not easily specified but of the fixed beds of uniform, simply-shaped particles: spheres, cylindrical beads. For the beds of these simple particles, the characteristic length is usually defined by the diameter d or 6V/S to characterize the heat transfer and/or pressure drop properties. However, it is difficult to define it for the porous materials of complex matrices such as foamed metal, fixed beds of nonumiform, irregularly shaped particles. Thus, in the cases of porous materials without enough knowledge on its fine structures, it is inevitable to carry out experiments to get informations on heat transfer and/or pressure drop characteristics. The aim of this paper is to predict the heat transfer characteristics from the pressure drop data because the heat transfer experiments are much more difficult.

There have been many works carried out on heat transfer (Dhingra[1], Dixon[2], Kudra[3]) or pressure drop characteristics of porous materials (Comite[4], Burke[5], Ergun[6]). However, works which concern both heat transfer and pressure drop characteristics simultaneously are rather scarce. Hamaguchi[7] adopted mean bore diameter as the characteristic length of the porous metal for pressure drop and mean fiber diameter for heat tarnsfer to yield fairly good correlations. If this choice of characteristic lengths is the best and no other alternative exists, no similarity rule is expected since the bore diameter and the fiber

* Department of Energy Conversion Engineering
** Toa Uinv. Shimonoseki 751, Japan
*** Kurume College of Technology, Kurume 830, Japan

diameter are independent. Unfortunately, the range of the experiments is not wide enough so that it is hardly examine the possibility of the existence of similarity rule from his data. Chiou[8] tried to define the characteristic length from the pressure drop data to correlate the heat transfer data with using it. This is very similar to our approach, however the results seem not to be good due to the mis-choice of the characteristic length as is discussed later.

In this paper, it is shown that a proper characteristic length is defined with which the Reynolds number Re and the Nusselt number Nu are defined. Then a universal law or a similarity rule $Nu = f(Re)$ applicable to various porous materials is derived.

2. Experimental apparatus and method

Experiments have been carried out with various porous materials. To measure the heat transfer coefficient suitable to each of them, two experimental apparatus were provided: one for steady state experiment and one for transient experiment. Details of the materials investigated are listed in **Table 1**.

Table 1. Characteristic dimensions of tested porous pieces

	Foamed metal		Wire gauge	
	#2	#4	A	B
ε (−)	0.952	0.965	0.868	0.946
a (mm^{-2})	15.0	76.3	10.9	3.34
b (mm^{-1})	0.250	0.715	0.745	0.308
l_1 (mm)	0.258	0.115	0.303	0.547
l_2 (mm)	4.00	1.40	1.34	3.24
c (−)	0.0645	0.0818	0.226	0.169
Specification	No. of cell (1/mm) (*)		Diameter of wire (mm) [22]	
	0.43~0.67	1.0~1.4	0.58	0.45

(*) Cermet, Sumitomo denko. Co

Particle	Glass sphere				Glass cylinder	Stylene sphere
	ϕ 4.2 (mm)		ϕ 2.5 (mm)		ϕ 3×5 (mm)	ϕ 1.4 (mm)
ε (−)	0.36	0.42	0.38	0.41	0.33	0.40
a (mm^{-2})	92.4	55.6	190	157	135	652
b (mm^{-1})	5.49	3.36	5.78	4.92	7.11	12.5
l_1 (mm)	0.104	0.134	0.0724	0.0796	0.0852	0.0392
l_2 (mm)	0.182	0.298	0.173	0.203	0.141	0.0800
c (−)	0.571	0.451	0.419	0.393	0.612	0.490

2.1 Steady state experiment

Experimental apparatus is shown in **Fig. 1**. The test section is a rectangular test porous plate (5 cm × 5 cm × 1 cm thick) heated by a current, which is mounted at the mouth of a 5 cm × 5 cm rectangular channel. Specifications of the tested porous pieces of foamed metal and of wire gauge are given by Kondoh[9]. The outside of the channel is wrapped with insulation layers and among them compensation heater is wound to minimize the heat loss. These are installed in a 14 cm dia., 4 mm thick copper tube. Sixteen alumel-chromel 0.1 mm dia. thermocouples are spot-welded on the surface of the elements of porous plate. Air intaken with a suction blower flows through the test section. Temperature distribution of air in the channel is measured with a sheathed thermocouple which is traversable radially. The heat transfer coefficient is evaluated from the heating power input and the mean temperature difference between the test plate and the flowing gas. The flow rate of air is measured with a rotameter and the pressure is with Shimazu micro-differential pressure meter at six axially distributed pressure taps; the pressure drop through the test section is estimated by linearly extrapolating these readings across the test section.

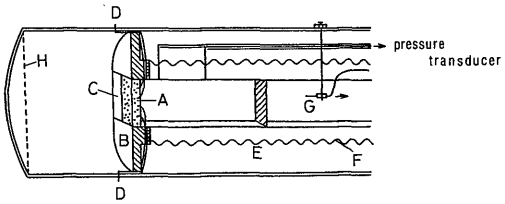

Fig. 1 Apparatus for the steady state experiment

Though the heat loss is minimized with the compensation heater, the conductive heat from test section through the bus bar is inevitable. This heat loss is estimated as follows. Relation between the heating power and the flow rate is experimentally obtained keeping the mean temperature of the test section constant. Then the curve is extrapolated to zero flow rate to give a value at an intersection, which is regarded as the heat loss $Q_{\mathrm{loss}}\ (T_s)$.

Experiments were carried out by increasing the air flow rate step by step with the heating power kept constant. Then, after the steady state is reached, temperatures and pressure drops are measured to obtain the volumetric heat transfer coefficient α_v defined by;

$$\alpha_v = q/\ (T_s - T_g), \tag{1}$$

$$q = (Q_{\mathrm{in}} - Q_{\mathrm{loss}})\ /AH. \tag{2}$$

2.2 Transient experiment

2.2.1 Experimental apparatus and method

Experimental apparatus is shown in **Fig. 2**. The test section is a 96 mm-diameter, 2 mm-thick acrylic cylinder in which a 60 mm-thick bed of glass beads to rectify the gas flow, a heater and a 100 mm-thick bed of test beads are set. The heater is two layers of Nichrome wires which are parallel-stretched, 10 mm apart with each other, and are heated electrically. Four kinds of test beads are used and each is filled up to two different porosities. Air is flown through this bed; its inlet temperature is heated stepwise and the

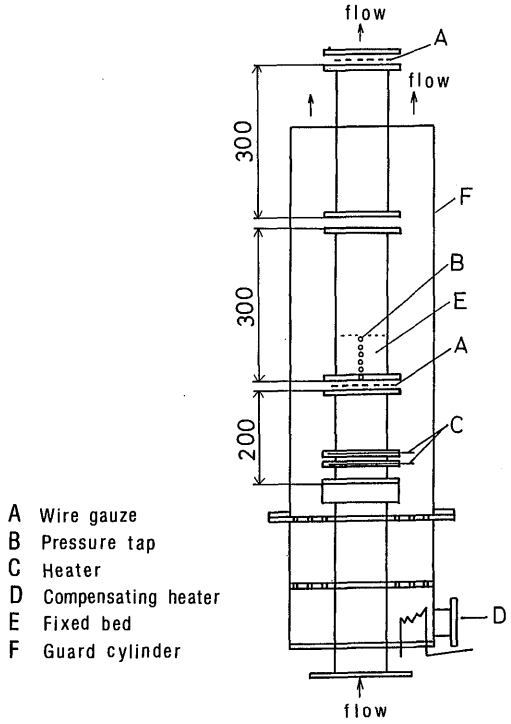

Fig. 2 Apparatus for the transient experiment

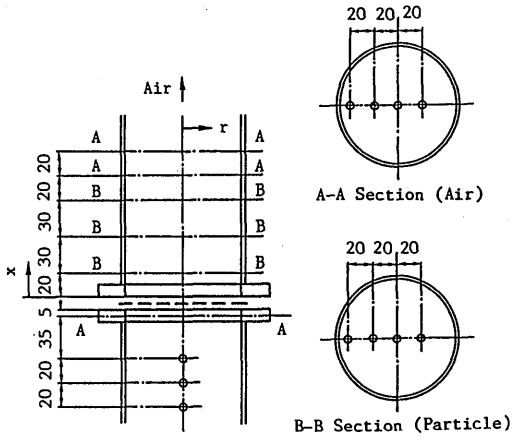

Fig. 3 Position of the temperature measurement

temperature response at each point in the bed is recorded. The whole of the test section is inserted in an outer acrylic cylinder. In the annulus gap between the inner and the outer cylinders a small of air, warmed slightly, is flown for thermal insulation.

For temperature measurement in the bed, some beads, with a 0.1 mm-dia. chromel-alumel thermocouple buried, are placed at bed heights 20, 50 and 80 mm at four radial positions (**Fig. 3**). Air temperature is measured at the inlet and at bed heights of 100 and 120 mm. These data are logged and processed with use of the temperature data logger YODAC-8 and the personal computer FM-7.

Pressure drop in the bed is measured with the Shimazu micro pressure differential meter at pressure taps located at the inlet, and at 20, 40, 60, 80, 100 and 120 mm from the inlet.

At a fixed flow rate, pressure drops are measured. Then the heating power is raised stepwise and the transient temperature variations are recorded at intervals of 10 − 60 sec. Experiments are carried out in the range of the initial gas temperature 16 − 28 deg C, final temperature 16 − 28 deg C and the gas flow rate 0.07 − 0.75 m/s.

2.2.2 Evaluation of volumetric heat transfer coefficient

Let air flow though a fixed bed at an initial temperature T. If the temperature of the gas at the inlet is changed stepwise, behaviors of temperature in its downstream as well as in the bed responding to it are described by a set of energy conservation equations.

Neglecting the heat transfer in radial direction, they are written for the bed;

$$(1-\varepsilon)\rho_p C_p \partial T_p/\partial t = \alpha_v (T_g - T_p) + (1-\varepsilon)\lambda_{eff}\partial^2 T_p/\partial x^2, \tag{3}$$

and for the gas;

$$\varepsilon \rho_g C_g \partial T_g/\partial t = -\alpha_v (T_g - T_p) - \rho_g C_g u_m \partial T_g/\partial x. \tag{4}$$

The boundary conditions are given by;

$$T_p = T_g = T_0 \quad \text{at } t = 0 \tag{5}$$

$$T_g = T_{\text{in}} \quad \partial T_p/\partial x = 0 \quad \text{at } x = 0 \tag{6}$$

$$\partial T_p/\partial x = 0 \quad \text{at } x = H \tag{7}$$

Though the heater input is raised stepwise, air temperature at the inlet of the bed is not of a step function due to the thermal capacity of the heater as well as to the time needed for the boundary layer around the heater to develop. It was found that the inlet temperature T_{in} was approximated by Fukuda[10];

$$(T_{\text{in}} - T_0)\ /\ (T_{\max} - T_0) = \theta + (1-\theta)\, t/t_{\max}\ (1 - e^{-t/t_0}), \tag{8}$$

where t_0 is a time constant of the heater and θ is defined from the experiment.

Once α_v is assumed Eqs. (3) ~ (8) are solved by the Laplace transformation method (Appendix). Comparing the analytical temperature transients with the experimental data, α_v was obtained as follows. Analytical and experimental data of nondimensional temperature were compared both in their values and slopes. (**Fig. 4**) Though the average velocity u_m is a known parameter measured in the experiment, u_m had to be dealt as an unknown one. This is presumably due to the existence of the radial distribution of the flow velocity, though the uniform onedimensional flow was assumed in the analysis. At it was found that the value of the nondimensional temperature was sensitive to α_v while the slope was to u_m, simultaneous evaluation of both α_v and u_m were possible. The obtained u_m to fit the data best was around 0.84 — 0.88 of the measured value in the case of 4.2 mm—dia. glass beads and 0.92 — 1.0 in the case of 2.5 mm-dia. glass beads. Results for α_v were examined in the later sections.

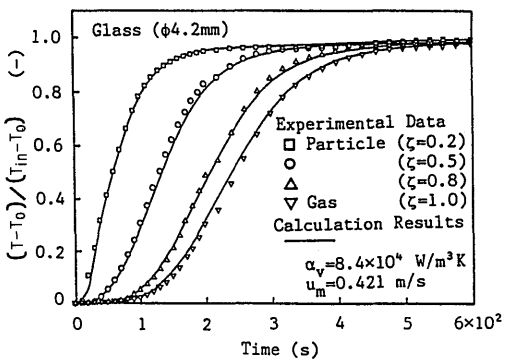

Fig. 4 Comparison of temperature transients between experimental and analytical prediction with properly chosen α_v and u_m.

3. Derivation of the similarity rule between heat transfer and pressure drop characteristics

3.1 Pressure drop characteristics

It is well known (Reynolds[11]) that the pressure drop in the porous bed is correlated by a quadratic equation;

$$\Delta P/H = a\mu_g u_m + b\rho_g u_m^2 \tag{9}$$

where the first term originates from the frictional resistance in the Poiseuille type viscous flow while the second from the kinetic energy losses in completely turbulent flow. In the limit of zero velocity, the first term in Eq. (9) dominates corresponding to the Darcy's law. For the packed bed of sphere beads Ergun's equation (Ergun[12]) is applicable, which is written as;

$$\begin{aligned} a &= 150(1-\varepsilon)^2/\varepsilon^3/d_p^2, \\ b &= 1.75(1-\varepsilon)/\varepsilon^3/d_p. \end{aligned} \tag{10}$$

According to the form of Eq. (9), it is obviously seen that there are two parameters with dimension of length which characterize the pressure drop of the porous beds, i. e.;

$$l_1 = 1/\sqrt{a}, \quad l_2 = 1/b. \tag{11}$$

By drawing a curve $\Delta p/H\mu_g u_m$ *vs* $\rho_g u_m/\mu_g$ we get 'a' from the intercept at zero velocity and 'b' from the slope. The way of combination of these two characteristic length to derive governing parameters (two at the most) is arbitrary and a typical set of parameters is either l_1 or l_2 and the ratio of these two;

$$c = l_1/l_2. \tag{12}$$

As far as the sphere beads, we found that the Ergun's equation was valid (**Fig. 5**) while it was not for other meterials tested. **Figure 6** shows the pressure drop data of the foam metal where it is clearly shown that the Ergun's equation is not applicable to correlate the data no matter how d_p is chosen. Therefore, in the general case of porous meterial with complicated structures, the characteristic length other than d_p should be properly chosen. Thus we are going to look for a similarity rule using the parameters: l_i ($i = 1$ or 2) as the characteristic length and a dimensionless parameter 'c'.

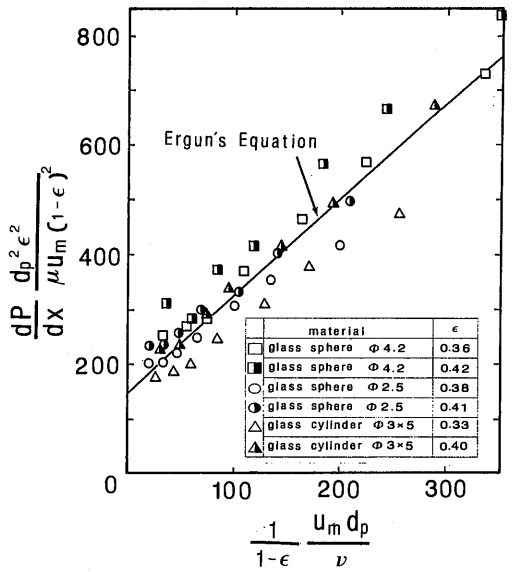

Fig. 5 Examination of Ergun's equation for sphere beads bed

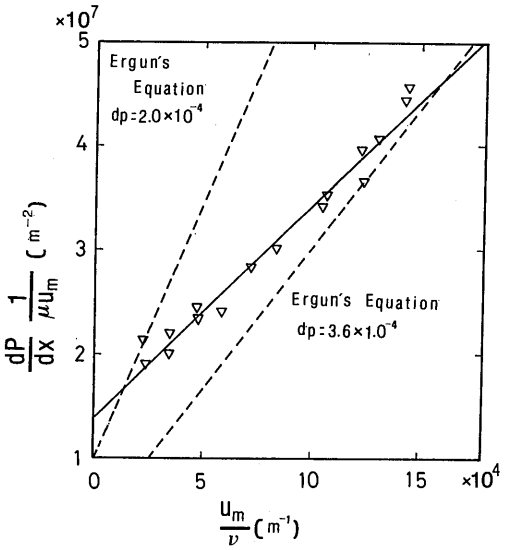

Fig. 6 Examination of Ergun's equation for foam metal bed

3.2 Heat transfer characteristics

Experimental data together with other available data are plotted in **Fig. 7**, where l_1 is chosen as the characteristic length for Re and Nu defined in Eqs. (13) and (14).

$$Nu = \alpha_v l_1^2/\lambda_g, \tag{13}$$

$$Re = u_m l_1/\nu_g. \tag{14}$$

This choice is arbitrary and it used to be the diameter of the sphere or the equivalent diameter defined by $d = 6V/S$ for packed beds of uniform beads in other works. The plot with l_2 as the characteristic length gave a similar trend, however it had a wider scattering than **Fig. 7**.

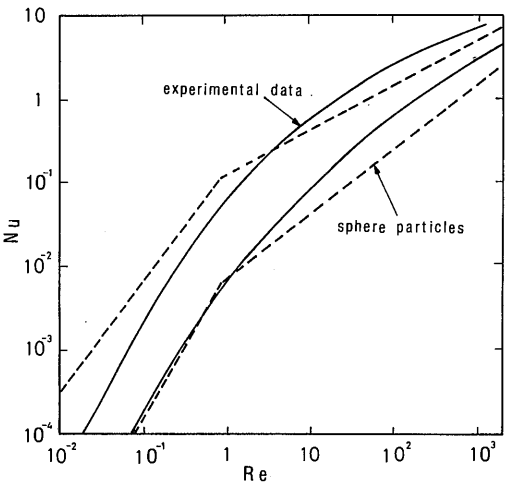

Fig. 7 Nu vs. Re with l_1 chosen as the characteristic length

To examine the validity of choosing l_1 as the characteristic length, experimental results for spherical beads by other researchers are compared in **Fig. 8**, where Eqs. (10) and (11) are used to evaluate l_1 for sphere beads. Since the heat transfer data for spheres are numerous (Ishimoto[13]) with wide scattering with each other, their rough envelope is drawn showing a general coincidence with our data.

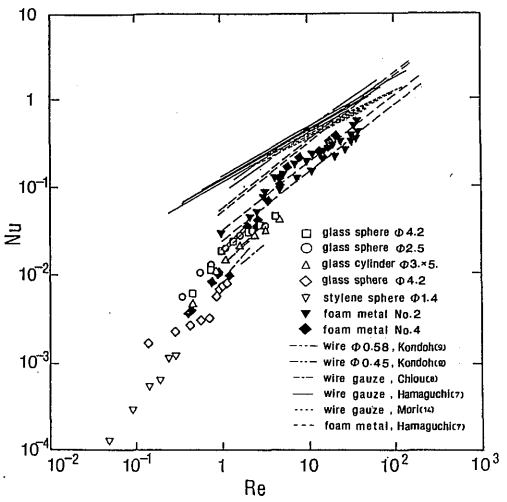

Fig. 8 Rough comparison between experimental results and the data for sphere beads bed by other researchers with l_1 chosen as the characteristic length

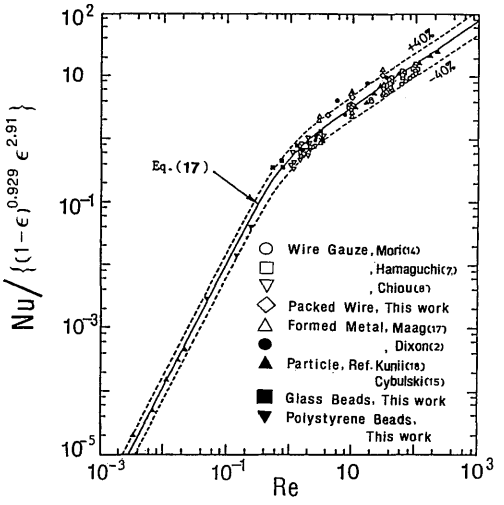

Fig. 9 Comparison between the similarity correlation (17) with the experimental data

Thus it is concluded that the heat transfer and the pressure drop are primarily correlated with l_1 as the characteristic length. However, slight diffences between the materials in **Fig. 7** should be explained with other parameters: ε, c, etc.

Now we examine an equation to correlate the heat transfer data in a general form;

$$Nu = K(1-\varepsilon)^m \varepsilon^n c^r (1-c)^s f(Re) \tag{15}$$

The exponents in Eq. (13) were obtained by the least square method to yield;

$$Nu = 0.430(1-\varepsilon)^{0.929} \varepsilon^{2.91} c^{0.795} Re^w,$$
$$w = 1.84 - 1.11 Re^{0.639}/(1 + Re^{0.639}). \tag{16}$$

It is interesting that each exponent is very close to integer. Since the effect of 'c' is negligible the important parameter among those we adopted first in Eqs. (11) and (12) is only l_1, and an alternative approximate equation without the term including 'c' is given by;

$$Nu = Nu'(1-\varepsilon)^{0.929} \varepsilon^{2.91}$$
$$Nu' = 0.9 Re^{1.95} (1 - \exp(-0.8 Re^{-1.27})). \tag{17}$$

In **Fig. 9** are plotted on Re vs. Nu' plane our data together with those of Mori[14], Hamaguchi[7] and Chiou[8] for wire nets and of Cybulski[15], Kunii[16] for fixed beads beds. The data given by Cybulski and Kunii are only for heat transfer and the characteristic

length l_1 are estimated from the Ergum's equation. It is shown that all of the data correlated by Eq. (17) within + 40%.

Conclusion

From the steady state and transient experiments, pressure drop as well as heat transfer data are taken for a variety of porous materials. Then the characteristic length is defined from the pressure drop data to correlate the heat transfer data. It is found that l_1, which characterizes the pressure drop of Poiseuille type viscous flow in the porous bed, does characterize the heat transfer data as well. Thus the similarity rule is confirmed to exist, which is presented with using l_1 as the characteristic length.

Acknowledgment

The authors would like to express their appreciations to Mr. T. Koda, Mr. S. Ishimoto, Mr. J. Matsuda, Mr. T. Katagami, Mr. K. Hirata, for their helps in the experiments and analyses, and to Mr. K. Nakagawa, for his assistance in manufacturing the facilities. This study is partly supported from research grant No. 63580182, sponsored by the Ministry of Education, Japan.

Nomenclature

a constant defined in Eq. (9)
A frontal area
b constant defined in Eq. (9)
c dimensionless parameter defined by Eq. (12)
C specific heat capacity
d equivalent diameter
H thickness of the bed
K constant
l_i $(i = 1, 2)$ characteristic length defined by Eq. (11)
Nu Nusselt number defined by Eq. (14)
ΔP pressure drop
q heat generation per volume
Q_{in} heat input
Q_{loss} heat loss
Re Reynolds number defined by Eq. (15)
S total heat transfer surface
t time
T temperature
u_m superficial velocity
V volume of the bed
x axial corrdinate

Greek symbols

α_v volumetric heat transfer coefficient
ε fractional void volume
ζ x/H
θ constant
λ thermal conductivity
μ visosity
ν kinetic visosity
ρ density

Subscripts

eff effective
g gas
max maximum
p particle.
s surface
0 initial.

Literature Cited

1) Dhingra, S. C., D. J. Gunn and P. V. Narayanan, Int. J. Heat Mass Transfer **27**, 2377-2385 (1984).
2) Dixon, A. G. and D. L. Cresswell, AIChE J. **25**(4), 663-676 (1979).
3) Kudra, T., A. S. Mujumdar and G. S. V. Raghavan, Int. Comm. Heat Mass Transfer **16**, 731-741 (1989).
4) Comite, J. and M. Renaud, Chem. Eng. Sci. **44**(7), 1539-1545 (1989).
5) Burke, S. P. and W. B. Plummer, Ind. Eng. Chem. **20**(11), 1196-1200 (1928).
6) Ergun, S. and A. A. Orning, Ind. Eng. Chem. **41**(6), 1179-1184 (1949).
7) Hamaguchi, K., S. Takahashi and H. Miyabe, Trans. Japanese Soc. Mech. Eng. **49**(445), 1991-2000 (1983); ibid **49**(445), 2001-2010 (1983).
8) Chiou, J. P. and M. M. El-Wakil, Trans. ASME, J. Heat Transfer, 69-76 (1966).
9) Kondoh, T., K. Fukuda, S. Hasegawa and K. Nakagawa, Eng. Sci. Reports, Kyusyu Univ., **9**(1), 57-63 (1987).
10) Fukuda, K., S. Hasegawa and T. Kondoh, Trans. Japanese Soc. Mech. Eng., **56**(529), 2729-2737 (1990).
11) Reynolds, O., Papers on mechanical and physical subjects, cambridge Univ. Press, (1900).
12) Ergun, S., Chem. Eng. Progress, **48**(2), 89-94 (1952).
13) Ishimoto, S., Eng. M. thesis, Kyusyu Univ., (1986).
14) Mori, Y. and H. Miyazaki, Trans. Japanese Soc. Mec. Eng., **33**(250), 956-964 (1967).
15) Cybulski, A., and M. J. Van Dalen, Chem. Eng. Sci., **30**, 1015-1018 (1975).
16) Kunii, D. and S. Smith, A. I. Ch. E. J., **7**(1), 29-34 (1961).
17) Maag, W. L. and W. F. Mattson, NASA TN D-3956, 1-20 (1967).
18) Kunii, D. and M. Suzuki, Int. J. Heat Mass Transfer **10**, 845-852 (1967).

Appendix

Equations (3) — (8) are rewritten in dimensionless forms with using the following variables;

$$\theta = \frac{T-T_0}{T_{\max}-T_0},\quad \zeta = \frac{x}{H},\quad \tau = \frac{t}{\rho_p C_p H^2/\lambda_{eff}}. \tag{A1}$$

Combining Eqs. (3) and (4) and Laplace transforming we have

$$\frac{g}{B}\frac{d^3\bar{\theta}_p}{d\zeta^3} + \left(1+\frac{\kappa s}{B}\right)\frac{d^2\bar{\theta}_p}{d\zeta^2} - g\left(1+\frac{s}{B}\right)\frac{d\bar{\theta}_p}{d\zeta} - \left((1+\kappa)s + \frac{\kappa s^2}{B}\right)\bar{\theta}_p = 0, \tag{A2}$$

where s is the parameter of the Laplace transformation, A denotes the Laplace transform of A and B, g, κ are defined by;

$$B = \frac{\alpha_v H^2}{(1-\varepsilon)\lambda_{eff}},\quad g = \frac{\rho_g C_g u_m H}{(1-\varepsilon)\lambda_{eff}},\quad \kappa = \frac{\rho_g C_g \varepsilon}{\rho_p C_p (1-\varepsilon)} \tag{A3}$$

If the routes of the characteristic equation of (A2) are given by Z_i $(i=1, 2, 3)$, θ_p is solved in a form:

$$\bar{\theta}_p = \sum_1^2 c_j e^{z_j \zeta}, \tag{A4}$$

where, C_i $(i=1, 2, 3)$ are solved from boundary conditions. In the same manner $\bar{\theta}_g$ is determined. Now, $\tilde{\theta}$ in the time domain is obtained by using the Crump's inverse Laplace transform method as follows;

$$\tilde{\theta}(\tau) = \frac{e^{\alpha\tau}}{\gamma}\left\{\frac{1}{2}\bar{\theta}(\alpha) + \sum_1^\infty \left\{Re\left\{\bar{\theta}(s_m)\cos\frac{m\pi\tau}{\gamma} - Im\left\{\bar{\theta}(s_m)\right\}\sin\frac{m\pi\tau}{\gamma}\right\}\right\}\right. \tag{A5}$$

$$E = e^{\alpha\tau}\sum_1^\infty \exp\left\{-\alpha(2n\gamma+\tau)\right\}\theta(2n\gamma+\tau), \tag{A6}$$

where $s_m = \alpha + (m\pi i)/\gamma$ and E is the measure of the error of this method defined by $\theta - \tilde{\theta}$. To obtain the converged solution α and γ should be appropriately taken which are chosen to be $\alpha = 10-150$, $\gamma = 1-1.5$ from the trial and error.